

Supplementary Materials for
Molecular Mechanism of Calcium Channel Regulation in the Fight-or-Flight Response

Matthew D. Fuller, Michelle A. Emrick, Martin Sadilek, Todd Scheuer,
William A. Catterall*

*To whom correspondence should be addressed. E-mail: wcatt@u.washington.edu

Published 28 September 2010, *Sci. Signal.* **3**, ra70 (2010)
DOI: 10.1126/scisignal.2001152

The PDF file includes:

Fig. S1. Inhibition of $\text{Ca}_v1.2\Delta1800$ channels by DCT.

Fig. S2. Modulation of $\text{Ca}_v1.2$ channel activity in single cells requires coexpression of AKAP15.

Fig. S3. Alanine substitutions have no effect on $\text{Ca}_v1.2\Delta1800$ channel activity in the absence of DCT.

Materials and Methods

References

Figure S1

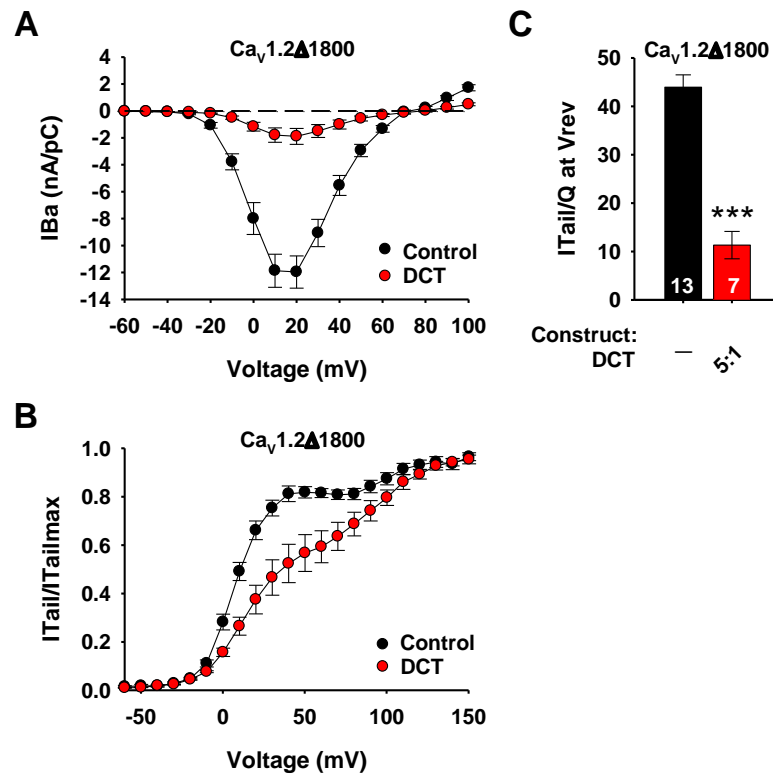


Figure S1. Inhibition of $Ca_V1.2\Delta1800$ channels by DCT.

(A) Current-voltage relationships for $Ca_V1.2\Delta1800$ channels in the absence and presence of DCT (5:1 cDNA molar ratio for transfection).

(B) Voltage-dependent activation curves for $Ca_V1.2\Delta1800$ channels in the absence and presence of DCT (5:1 cDNA molar ratio for transfection).

(C) Ratio of charge to tail current amplitude at the reversal potential (coupling efficiency) (nA/pC) for $Ca_V1.2\Delta1800$ channels in the absence and presence of DCT. *** $P < 0.001$ vs $Ca_V1.2\Delta1800$. N values and mean \pm SEM are indicated.

Figure S2

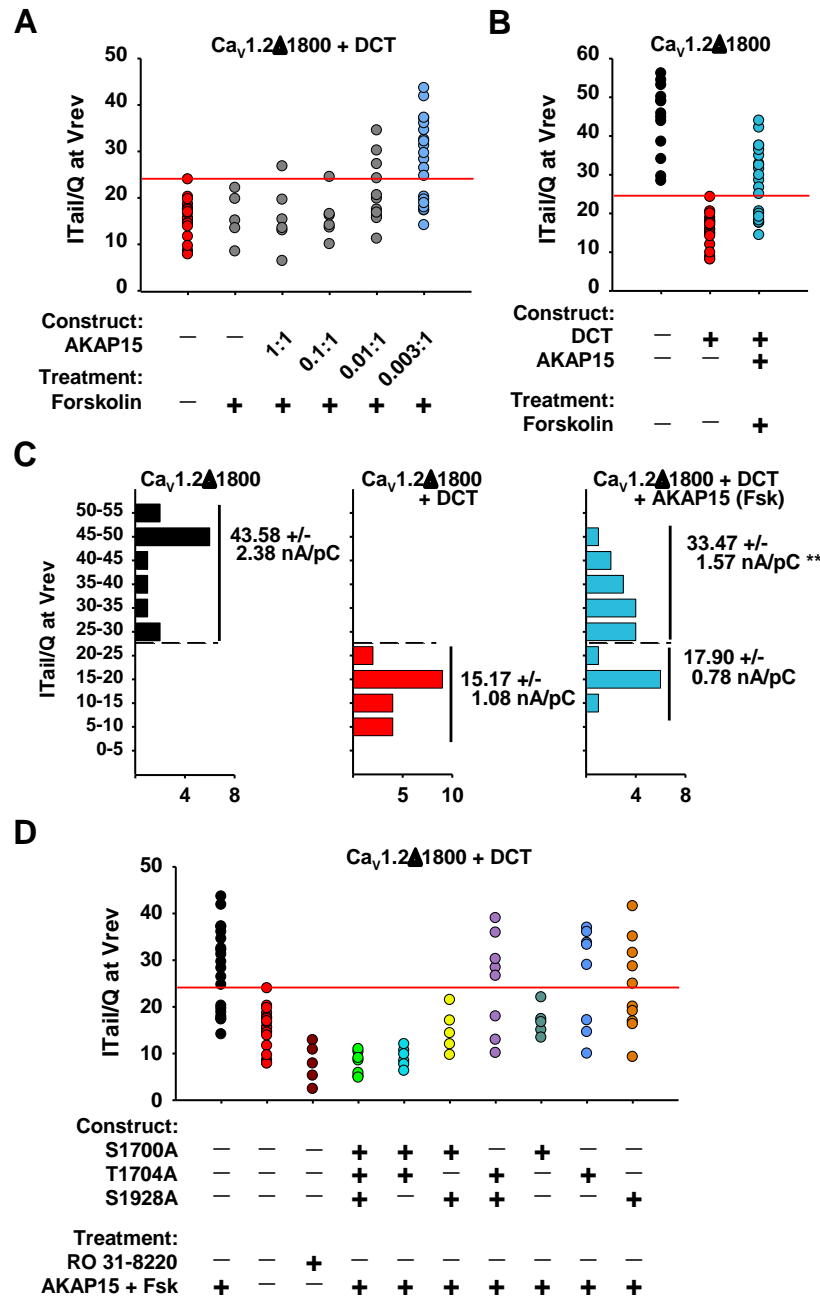


Figure S2. Modulation of Ca_v1.2 channel activity in single cells requires coexpression of AKAP15.

(A) Coupling efficiency of individual experiments for Ca_v1.2Δ1800+DCT with varying ratios of AKAP15: Ca_v1.2Δ1800 in the absence and presence of 5 μM forskolin (Fsk). Red horizontal line indicates the maximum current observed with Ca_v1.2Δ1800+DCT channels.

(B) Coupling efficiency measurements for individual experiments for $\text{Ca}_v1.2\Delta1800$ channels without or with AKAP15 (0.003:1) in the absence and presence of 5 μM forskolin. Red horizontal line indicates the maximum current observed with $\text{Ca}_v1.2\Delta1800+\text{DCT}$ channels.

(C) Binned coupling efficiency measurements for experiments shown in B. ** $P < 0.01$ vs $\text{Ca}_v1.2\Delta1800$.

(D) Coupling efficiency (individual measurements) for wild-type $\text{Ca}_v1.2\Delta1800+\text{DCT}$ channels in the absence or presence of 1 μM RO 31-8220, or wild-type or alanine-substituted $\text{Ca}_v1.2\Delta1800+\text{DCT}$ channels with AKAP15 and 5 μM forskolin. Red horizontal line indicates the maximum current observed with $\text{Ca}_v1.2\Delta1800+\text{DCT}$ channels.

Figure S3

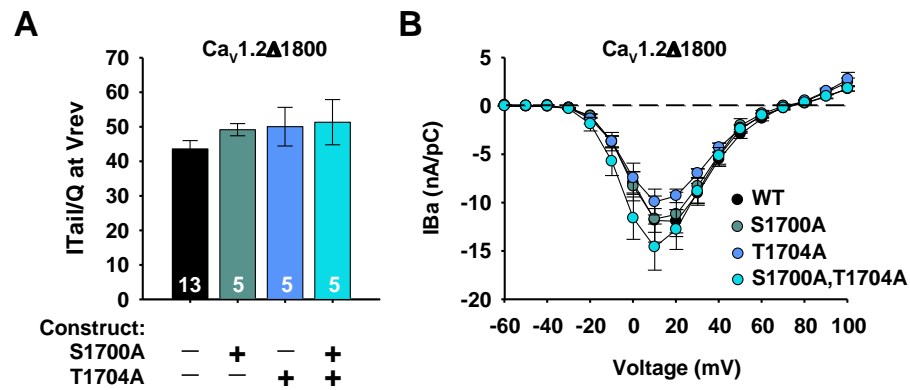


Figure S3. Alanine substitutions have no effect on $\text{Ca}_v1.2\Delta1800$ channel activity in the absence of DCT.

(A) Coupling efficiency (nA/pC; mean \pm SEM) for wild-type $\text{Ca}_v1.2\Delta1800$ channels or $\text{Ca}_v1.2\Delta1800$ channels with alanine substitutions at Ser¹⁷⁰⁰ or Thr¹⁷⁰⁴.

(B) Current-voltage relationships (mean \pm SEM) for wild-type $\text{Ca}_v1.2\Delta1800$ channels or $\text{Ca}_v1.2\Delta1800$ channels with alanine substitutions at Ser¹⁷⁰⁰ or Thr¹⁷⁰⁴.

N values and mean \pm SEM are indicated.

Supplementary Materials and Methods

Antibodies and cDNA constructs

Rabbit polyclonal antibodies were generated as described previously against peptides corresponding to rabbit Ca_v1.2 residues ⁸²¹TKINMDDLQPNESEDKS (T, Thr; K, Lys; I, Ile; N, Asn; M, Met; D, Asp; L, Leu; Q, Gln; P, Pro; E, Glu) in the intracellular loop between domains II and III for anti-Ca_v 1.2, or residues ¹⁹²³LGRRApSFHLECLK (G, Gly; R, Arg; F, Phe; H, His; C, Cys) in the distal C-terminus for anti-pS1928 as described (1). Constructs used in this study include rabbit α₁1.2a (2), rat β_{1b} and β_{2b} (3, 4), rabbit α₂δ₁ (5), AKAP15 (6), PKA-Cα (7) and PKA-RIIα (8) in pcDNA3 and CaM KIIN in pJPA7 (9).

tsA-201 Cell Culture and Transfection

For biochemical studies: tsA-201 cells were cultured in DMEM/Ham's F12 supplemented with 10% FBS and 100 units/mL penicillin and streptomycin. Cells were grown to ~70% confluence in 10% CO₂ and transiently transfected with cDNAs encoding α₁1.2a, β_{1b}, and α₂δ₁ subunits at a 1:1:1 molar ratio using the Fugene 6 method (Roche). Twenty-four hours post-transfection, cells were washed with PBS, drug treated as indicated, and membranes were collected and solubilized. For electrophysiological studies: tsA-201 cells were grown in similar conditions and transfected with cDNAs encoding full-length, truncated, or mutant α₁1.2a, β_{1b} or β_{2b}, α₂δ₁ at a 1:1:1 molar ratio using Fugene 6. Wild-type or mutant distal₁₈₀₁₋₁₂₇₁ constructs were transfected with truncated α₁1.2a channels using varying molar ratios ranging from 0.25:1 to 5:1 (distal₁₈₀₁₋₂₁₇₁ cDNA: truncated α₁1.2a). In addition a 10-fold lower molar concentration of cDNA encoding eGFP in pcDNA3 was added to each transfection mixture as an indicator of transfection efficiency.

Membrane Preparation for Immunoblot Analysis

Twenty-four hours after transfection, cells were washed with PBS, treated with 10 μ M forskolin, 5 μ M ionomycin (Sigma), 1 μ M okadaic acid (Calbiochem), 10 nM cyclosporine A (Calbiochem) for 10 min, or with 1 μ M cell permeable autocamtide-2 related inhibitor peptide II (Calbiochem) for 45 min, and scraped into 1.4 mL of ice cold 1x bRIA (10 mM Tris pH 7.4, 100 mM NaCl, 1 mM EGTA, 5 mM EDTA containing 1x Protease Inhibitor Complete cocktail (Roche), 0.5 mM sodium vanadate, 1 μ M okadaic acid, and 10 nM cyclosporin A). Cells were lysed, nuclei were pelleted by centrifugation, and supernatant was collected and centrifuged to pellet microsomal membranes. The membrane was solubilized in 500 μ L 1x bRIA containing 0.5% Triton X-100 for 30 min end-over-end at 4 °C. Insoluble material was removed by centrifugation, 50 μ L of soluble membrane was separated by SDS-PAGE (8-16% gradient gel from Invitrogen), and transferred to a nitrocellulose membrane. Blots were probed with indicated antibodies at 1:100 dilution using standard procedures.

Expression and Purification of GST-tagged Cav1.2 C-terminus

pCOOL GST-rabbit Cav1.2(1670-1731) was transformed into BL21-STAR *E. coli* (Invitrogen). Protein was prepared from 100 mL culture (Luria broth, 100 μ g/mL ampicillin) induced for 2 h at 30 °C, and purified using GST-Sepharose (Amersham) by standard procedures. Protein was eluted in storage buffer [(mM) 10 Tris pH 7.5, 100 NaCl, 1 DTT] with 20 mM glutathione (pH 8.0), and dialyzed into storage buffer. Pure protein was snap frozen in liquid nitrogen and stored at -80 °C in single use aliquots. GST- Cav1.2(1670-1731) (2.5 μ g) was phosphorylated by 100 U PKA (Sigma, from Bovine heart), 100 U CaMKII (New England Biolabs), or 25 U CK2 (New

England Biolabs) for 2.5 h at 30 °C in assay buffer [(mM) 20 Tris pH 7.5, 10 MgCl₂, 2 DTT, 10 NaCl, 200 ATP]. Reactions were quenched, proteins were resolved by SDS-PAGE, subjected to in-gel trypsin digestion (Gold, Promega; 10), and phosphate incorporation was assessed by mass spectrometry. Mass spectrometry was performed using an Agilent 1100 series capillary HPLC (Agilent Technologies) coupled to an LCQ Classic ion trap mass spectrometer (ThermoElectron). Peptides were loaded onto a Paradigm Platinum Peptide Nanotrap (Michrom Bioresources), then separated on a reverse-phase capillary column (10 cm x 75 μm, Jupiter Proteo C12, Phenomenex) with a linear gradient from 2%-40% acetonitrile in 40 min. One full mass scan was acquired (300-2000 Da) and the four most intense peaks were selected for MS/MS analysis. The dynamic exclusion limit was set to exclude a given m/z after it had been sequenced 2x during a 90 s interval. Mass spectra were analyzed using TurboSequest configured with the following parameters: a peptide mass tolerance of 2.5 Da (avg), a fragment ion mass tolerance of 1.0 Da (avg), differential modification on S/T/Y +80 Da, and allowance of two incomplete cleavages. All MS/MS peak assignments were manually validated. The relative abundance of the modified forms for each peptide was determined using the ICIS peak detection method for the indicated extract ions. The percentages were calculated based on the sum of integrated peak areas for all detected modified forms of the peptide.

Electrophysiology

Twenty-four hours post-transfection, cells were plated at low density and recordings were made 38–48 h post-transfection using the whole-cell configuration of the patch clamp technique. Patch pipettes (1.5–2 MΩ) were pulled from micropipette glass (VWR Scientific, West Chester, PA, USA) and fire-polished. Currents were recorded with an Axopatch 200B amplifier (Axon

Instruments Inc., Union City, CA, USA) and sampled at 5 kHz after anti-alias filtering at 2 kHz. Data acquisition and command potentials were controlled by either pCLAMP or HEKA Pulse software and data were stored for later off-line analysis. Voltage protocols were delivered at 10 s intervals, and leak and capacitive transients were subtracted using a *P/4* protocol. Approximately 80% of series resistance was compensated with the patch clamp circuitry. The extracellular bath solution contained (mM): 150 Tris, 10 glucose, 1 MgCl₂ and 10 BaCl₂ (adjusted to pH 7.4 with MeSO₄). The intracellular solution contained (mM): 135 CsCl₂, 10 EGTA, 1 MgCl₂, 4 MgATP and 10 Hepes (pH 7.3, adjusted with CsOH) (11).

Analysis of Electrophysiological Recordings of Ca_v 1.2 Channels

Current–voltage relationships from peak inward Ba²⁺ currents were normalized to gating charge (*Q*) to correct for variation in protein abundance. Gating currents result from the voltage-driven movement of gating charges as conformational changes occur preceding channel opening and are independent of channel unitary conductance and open probability (*P*_o). Gating charge movement was measured by applying a series of test pulses at 10 s intervals from the holding potential of -80 mV to potentials between +60 mV and +80 mV in 2mV increments and integrating the gating charge movement at the reversal potential for the ionic current. The ionic current gives a functional readout that includes the number of open channels, the single channel conductance, and channel *P*_o during the depolarizing step. By comparing the ionic and gating currents we determined the efficiency of coupling of the charge movement of the voltage sensors to the subsequent opening of the pore by calculating the ratio of tail current to gating charge [tail current (nA)/ integrated gating charge (pC)]. Tail currents were recorded after repolarization to -50 mV following each test pulse.

Structural Modeling of the PCRD-DCRD Interaction

Structural modeling of the PCRD and DCRD was performed as described (10).

Supplementary References

1. K.S. De Jongh, B.J. Murphy, A.A. Colvin, J.W. Hell, M. Takahashi, W.A. Catterall, Specific phosphorylation of a site in the full-length form of the alpha 1 subunit of the cardiac L-type calcium channel by adenosine 3', 5'-cyclic monophosphate-dependent protein kinase. *Biochemistry* **35**, 10392-10402 (1996).
2. A. Mikami, K. Imoto, T. Tanabe, T. Niidome, Y. Mori, H. Takeshima, S. Narumiya, S. Numa, Primary structure and functional expression of the cardiac dihydropyridine-sensitive calcium channel. *Nature* **340**, 230-233 (1989).
3. M. Pragnell, J. Sakamoto, K.P. Campbell, Cloning and tissue-specific expression of the brain calcium channel β subunit. *FEBS Lett.* **291**, 253–258 (1991).
4. R. Hullin, D. Singer-Lahat, M. Freichel, M. Biel, N. Dascal, F. Hofmann, V. Flockerzi, Calcium channel beta subunit heterogeneity: functional expression of cloned cDNA from heart, aorta and brain. *EMBO J.* **11**, 885-890 (1992).
5. S.B. Ellis, M.E. Williams, N.R. Ways, R. Brenner, A.H. Sharp, A.T. Leung, K.P. Campbell, E. McKenna, W.J. Koch, A. Hui, A. Schwartz, M.M. Harpold, Sequence and expression of mRNAs encoding the α 1 and α 2 subunits of a DHP-sensitive calcium channel. *Science* **241**, 1661-1664 (1988).
6. P.C. Gray, B.D. Johnston, R.E. Westenbroek, L.G. Hays, J.R. Yates 3rd, T. Scheuer, W.A. Catterall, B.J. Murphy, Primary structure and function of an A kinase anchoring protein associated with calcium channels. *Neuron* **20**, 1017-1026 (1998).

7. M.D. Uhler, G.S. McKnight, Expression of cDNAs for two isoforms of the catalytic subunit of cAMP-dependent protein kinase. *J. Biol. Chem.* **262**, 15202-15207 (1987).
8. G. Cadd, G.S. McKnight, Distinct patterns of cAMP-dependent protein kinase gene expression in mouse brain. *Neuron* **3**, 71-79 (1989).
9. B.H. Chang, S. Mukherji, T.R. Soderling, Characterization of a calmodulin kinase II inhibitor protein in brain. *Proc. Natl. Acad. Sci. USA* **95**, 10890-10895 (1998).
10. <http://donatello.ucsf.edu/ingel.html>; Gold, Promega
11. J.T. Hulme, V. Yarov-Yarovoy, T.W. Lin, T. Scheuer, W.A. Catterall, Autoinhibitory control of the Ca_v1.2 channel by its proteolytically processed distal C-terminal domain. *J. Physiol.* **576**, 87-102 (2006).